

<https://doi.org/10.18524/1810-4215.2025.38.344822>

PREPARING RADIO AND OPTICAL DATA FOR COMPARING BINARY BLACK HOLE CANDIDATES: THE CASE OF OJ 287

D. A. Zabora^{1,2}, M. I. Ryabov², A. L. Sukharev²

¹ Odesa I. I. Mechnikov National University,
Odesa, Ukraine, zaboradaniil@gmail.com

² Institute of Radio Astronomy of the National Academy of Sciences of Ukraine (IRA NASU),
Kharkiv, Ukraine, rian@rian.kharkov.ua

ABSTRACT.

Background. In light of recent discoveries, in particular the appearance in the literature of strong evidence in favor of a binary supermassive black hole (SMBH) in the core of OJ 287, interest in the search for such objects has revived. Therefore, the issue of detecting candidates has gained considerable relevance. The variability of the radio flux of Active Galactic Nuclei (AGN) in the optical, radio and spatial dimensions provides significant insights into the complex structure of physical phenomena in the immediate vicinity of the black hole and the conditions for launching jets. In particular, these manifestations may indicate the presence of a binary SMBH in the center of such a system.

Data & methods. The paper uses multi-filter optical observations (aggregated by AAVSO) and radio observations of the MOJAVE project at 15 GHz, given in Lister et al. (2019), in the form of radio fluxes and bright component positions (obtained from the VizieR database). Time-frequency analysis methods (including wavelet analysis, LombScargle, and cross-correlation) as well as clustering and regression methods of machine learning and analysis are used for processing.

Results. The intersections of the accretion disk by the companion black hole in the core of OJ 287 cause characteristic optical flares and affect the jet morphology. The latter is manifested in the change in the angles of the bright features (components). It is found that these changes in the case of OJ 287 exhibit noticeable patterns that can be used as indicators for binary black hole candidates (SMBBHs) in active nuclei.

Conclusions. The established connection between optical flares (with potential X-ray verification) and changes in the orientation of jet components with a characteristic pattern can serve as a criterion for detecting binary black hole candidates in AGN.

Keywords: binary supermassive black hole (BSMBH), AGN, blazar, optical flares, jet morphology, quasi-periodicity.

АНОТАЦІЯ.

Передісторія. У світлі нещодавніх відкриттів, зокрема появу у літературі вагомих доказів на користь подвійної надмасивної чорної діри (SMBH) у ядрі OJ 287, інтерес до пошуку подібних об'єктів пожвавився. Відтак, питання виявлення кандидатів набуло значної актуальності. Змінність радіопотоку Активних ядер галактик (АЯГ) в оптичному, радіота просторовому вимірах надає суттєві інсайти стосовно складної структури фізичних явищ у безпосередньому оточенні чорної діри та умов запуску джетів. Зокрема, ці прояви можуть свідчити про наявність подвійної SMBH у центрі такої системи.

Дані та методи. У статті використовуються багатофільтрові оптичні спостереження (агреговані AAVSO) та радіоспостереження проекту MOJAVE на частоті 15 GHz, наведені в Lister et. al. (2019), у вигляді радіопотоків та положень яскравих компонент (отриманих із бази VizieR). Для обробки застосовуються методи часово-частотного аналізу (зокрема вейвлет-аналіз, LombScargle та крос-кореляція), а також кластеризаційні та регресійні методи машинного навчання та аналізу.

Результати. Перетини акреційного диску чорною дірою-компаньоном у ядрі OJ 287 спричиняють характерні спалахи у оптичному діапазоні та впливають на морфологію джета. Останнє виявляється у зміні позиційних кутів яскравих особливостей (компонент). Виявлено, що ці зміни у кейсі OJ 287 демонструють помітні патерни, які можна використовувати як індикатори для кандидатів на подвійну SMBH у активних ядрах.

Висновки. Встановлений зв'язок між оптичними спалахами (з потенційною рентгенівською верифікацією) та змінами орієнтації компонентів джетів із характерним патерном може слугувати критерієм виявлення кандидатів у подвійні чорні діри в АЯГ.

Ключові слова: подвійна надмасивна чорна діра, АЯГ, блазар, оптичні спалахи, морфологія джета, квазіперіодичність.

1. Introduction

Active Galactic Nuclei (AGN) are objects located in the central regions of some galaxies and are characterized by extreme luminosity in almost the entire wavelength range: from radio waves to gamma rays, which makes them one of the most powerful sources of electromagnetic radiation in the Universe. According to the current Standard Model (Marscher, 2009), energy supply is provided by the release of gravitational and rotational energy as a result of the accretion of matter onto a supermassive black hole in the center.

The accretion disk surrounding a supermassive black hole is the primary source of optical and ultraviolet radiation. In it, matter falling onto the black hole is heated to high temperatures, releasing gravitational energy in the form of the electromagnetic continuum.

Surrounding the disk is a dust torus, a structure of cooler matter that partially shields the central region. The torus intercepts some of the ultraviolet and optical radiation, heats up, and radiates in the infrared range, forming the characteristic IR component of the spectrum.

Many active nuclei exhibit relativistic jets, collimated plasma streams ejected from the black hole's surroundings in directions close to the polar axis (perpendicular to the disk plane) and observed at distances of tens to hundreds of kpc from the nucleus. These jets emit in a wide range of wavelengths, from radio to X-rays, as a result of synchrotron and inverse Compton processes.

It is possible that the supermassive black hole at the center of a galactic system is not a single one, but multiple—for example, a double or even a triple. According to recent studies, this is exactly the configuration exhibited by the object OJ 287, which is considered one of the most convincing candidates for the presence of a double supermassive black hole.

OJ 287 is classified as a BL Lacertae object, a high-luminosity type of AGN with a relativistic jet directed almost into the observer's line of sight, resulting in significant Doppler beaming and making the object very bright despite its considerable distance. It is located at a cosmological distance corresponding to a redshift of $z = 0.3056$ (ASA/IPAC Extragalactic Database, 2008) in the constellation Cancer. OJ 287 is exceptional in its proximity to the ecliptic plane (it has been accidentally captured on a large number of photographic plates) and, as a result, in the unprecedentedly long series of historical observational data available: over 120 years (Alachkar et al., 2023), which is critical for identifying long-term orbital effects.

The initial hypothesis of the presence of a double SMBH in the OJ 287 system first appeared in Sillanpää et al. (1988), where periodic flares (~ 11.65 yr) were observed in the optical curve of the AGN. They

were associated with a tidal perturbation of the accretion disk of the primary BH by the companion as it passed the pericenter. This perturbation would cause increased accretion towards the center and would lead to a flare in the optics. The masses of the companions were estimated at $\sim 5 \cdot 10^9 M_\odot$ and $\sim 2 \cdot 10^7 M_\odot$, with a semi-major axis of ~ 0.1 pc. The lifetime of such a system (due to the energy loss to gravitational radiation) was also estimated to be $\sim 10^5$ yr. The observed pattern allowed for the prediction of the outburst, which was later confirmed in 1994.

Further development (or even rethinking of the model), which is already closer to modern ideas, is presented in the Lehto and Valtonen (1996). In it, the authors noticed that: the flares are not strictly periodic—the time intervals between them change; the structure of the flares is often double (two peaks separated by an interval of 1–2 years); the change in the brightness of the base level and the flares hinted at the modulation of the light curve with a period of 60 years. Another mechanism has been proposed: the flares arise as a result of the collision of a secondary black hole (moving at an angle to the accretion disk) with the radiation-dominated optically thick and geometrically thin accretion disk of the primary at supersonic speed (twice per period), which leads to a shock wave at the collision site, the subsequent formation of optically thick hotter bubbles, their cooling and bremsstrahlung radiation (which are observed as flares); a relativistic precession of the secondary's orbital semi-axis and the amplification of the flares by gravitational waves have been introduced (to explain their irregularity). The following parameters were refined: the eccentricity of the secondary black hole's orbit (0.685), the orbital period (~ 12.07 yr), an upper estimate of the decay rate of the orbital period ($\sim 10^{-3}$), the precession period of the system's semi-major axis (130 years), and the properties of the accretion disk.

Sundelius et al. (1997) performed a multi-particle simulation of the disk within the framework of a restricted three-body problem with previously calculated BH orbits: large outbursts were identified with the passage of the pericenter by the companion black hole and induced mass flows from the perturbed accretion disk to the main black hole. Superflares superimposed on longer outbursts are associated with the crossing of the accretion disk by the companion (as in Lehto and Valtonen, 1996). The gas perturbed by the shock wave leaves the disk for a certain time, after which it cools to a temperature at which it becomes capable of radiating. This causes a delay between the moment of impact and the appearance of the optical flare. As a result, the model allowed the authors to calculate the onset of the 1995 superflare quite accurately. The simulation reproduced with good accuracy slow flares (~ 1 yr) associated with the increase in the accretion period and faster ones

(~ 0.1 yr) associated with the crossing of the accretion disk, as well as brightness modulation (60-year cycle) associated with the precession of the semi-major axis and strong flares (when the companion's semi-major axis was almost perpendicular to the disk).

Subsequent works (Valtonen and Lehto, 1997, Valtonen et al. 2006, 2010, 2016, Dey et al., 2019) showed the importance of taking into account gravitational waves and the associated energy losses, expanded the model to take into account the spin of black holes and spin-orbit interaction, and refined the model parameters: the mass of the primary black hole $\sim 18.35 \cdot 10^{10} M_{\odot}$, the mass of the secondary black hole $\sim 150 \cdot 10^6 M_{\odot}$, the Kerr parameter for the primary BH $\chi_1 \sim 0.381$, the eccentricity of the orbit ~ 0.657 , the period ~ 12.06 yr, etc. As a result, a super-accurate prediction of the flare caused by the intersection of the accretion disk was observed by the Spitzer telescope in 2019 with an accuracy of up to 4 hours (Laine et al., 2020).

In general, we are talking about tidally induced outbursts, which are associated with the influence of a secondary black hole, which manifests itself in the destabilization of the accretion disk (especially when it passes the pericenter), accelerating the accretion rate and can last for years; and shock flares - sharp short-lived and powerful events (flares and superflares) associated with crossings of the accretion disk twice (once on the way to the pericenter and once after per orbital cycle) with an interval of about a year between flares and subsequent afterflares in the jet in ~ 2 months.

Table 1: Summary table of OJ 287 activity events

Date	Description	References
Nov 1995 – Jan 1996	The second flare of the 1994–1996 pair	Sillanpaa et al. (1996)
2005 – 2008	Tidal-induced period of activity	Valtonen et al. (2009)
Nov 2005	First flare from 2005-2008	Valtonen et al. (2006)
Sep 2007	Second flare from 2005-2008 (giant flare)	Valtonen et al. (2009)
Nov 2015	First flare from 2015-2019	Valtonen et al. (2016)
Oct 2016	Unexpected double flare recorded in X-rays and optics explained as disk afterflare	Komossa et al. (2021)
Jul 2019	Second flare from 2015-2019	Laine et al. (2020)

We are interested in events in the period 1995–2020, for which there is data on the movement of bright components in jets, so will provide a table of activity events with their descriptions and links (Table 1.).

2. Data and methods

This paper uses AAVSO and MOJAVE data to highlight the connection between optical and radio flares and changes in the morphology of the OJ 287 jet. AAVSO (American Association of Variable Star Observers) is an international non-profit organization that brings together professional and amateur astronomers to coordinate observations of variable stars and other astronomical objects. The corresponding AAVSO International Database is one of the largest archives of photometric observations. MOJAVE (MOJAVE Team, 2025, Lister et al., 2018) is a program of long-term monitoring observations of AGN jets using the VLBA radio interferometer. The MOJAVE project also has an open database (MOJAVE/2cm Survey Data Archive) for a sample of over 500 AGN, which provides access to radio fluxes, radio images of nuclei and jets, polarization maps, and data on the positions of bright components in jets with time intervals ranging from 5-10 days to a year between observation sessions.

In particular, the work uses data on radio fluxes (Fig. 1) and positions (Fig. 2) of bright components in the MOJAVE project jets with a resolution of up to 0.47 mas at a frequency of 15 GHz, which are presented in works of Lister et. al. (2019, 2021) and obtained from the VizieR database (Ochsenbein, 1996).

Previous works related to the study of AGN using MOJAVE data are presented in works of Zabora et al. (2022, 2023) and Zabora, Ryabov, and Sukharev (2025), which investigate the variability of radio fluxes and spatial variability of jet morphology of AGN samples.

As can be seen, the available data is in the range from 1995-04-07 to 2019-06-29, accordingly (despite the significantly longer duration of the time series), the AAVSO data was taken for the same interval (Fig. 3).

The most complete are the observations in the Johnson V filter, but they are often missing on key event dates. To ensure maximum completeness of the time series, we also include data from other photometric filters — Johnson B, Cousins I and R, Sloan i, r, g, etc.

Since we are primarily interested in the shape of the light curve during the flare, rather than the absolute magnitude values, we convert all observations to the Johnson V scale. Typically, this conversion requires color indices and spectral approximations that take into account the physical properties of the source. However, in our case, absolute accuracy is not critical—it is the structure of the light curve that matters.

Therefore, we build separate regression models of the

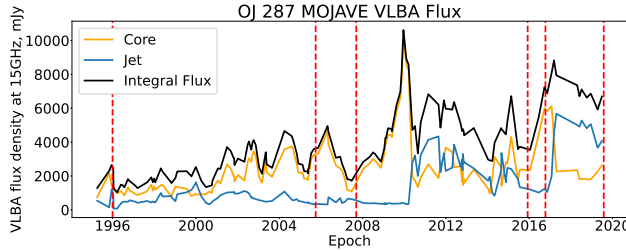


Figure 1: Radio fluxes of the core (orange), jet (blue), and total (black)

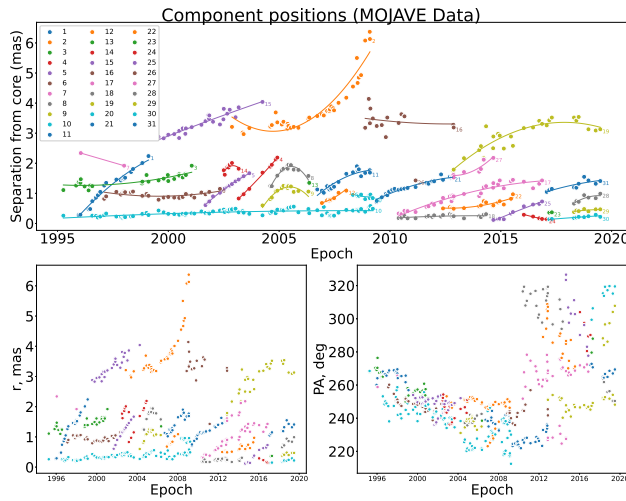


Figure 2: Position of bright components over time: sep vs time plot, distance from nucleus in mas (bottom left) and position angles in degrees (bottom right)

transition from each filter to Johnson V, independently of the others. This allows us to use even single observations on individual dates when only one filter is available, and to preserve maximum temporal density for subsequent paternization.

Fortunately, the physical nature of the emission can be partially accounted for by constructing these calibration models based on data from OJ 287 itself — using those dates for which simultaneous observations are available in Johnson V and the corresponding alternative filter. For now, we limit ourselves to simple linear models and to moving from each alternative filter to Johnsons V separately, but in the future this approach can be refined or expanded (by taking into account approximated observations in additional filters and using real ones where they are available). A comparison of observations in other filters and Johnsons V, as well as regression model metrics, is given in Fig. 4, the full light curve is given in Fig. 5, and its wavelet periodogram is given in Fig. 6.

To analyze the temporal structure of periodicity in

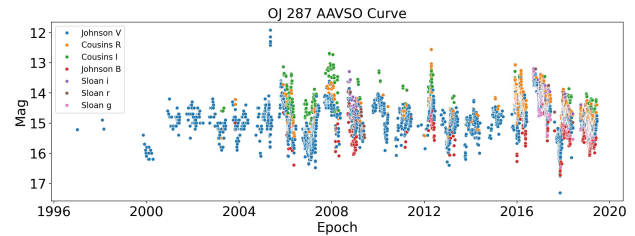


Figure 3: Light curve according to AAVSO data in Johnson V, B, Cousins I, R, B, Sloan i, r and g filters

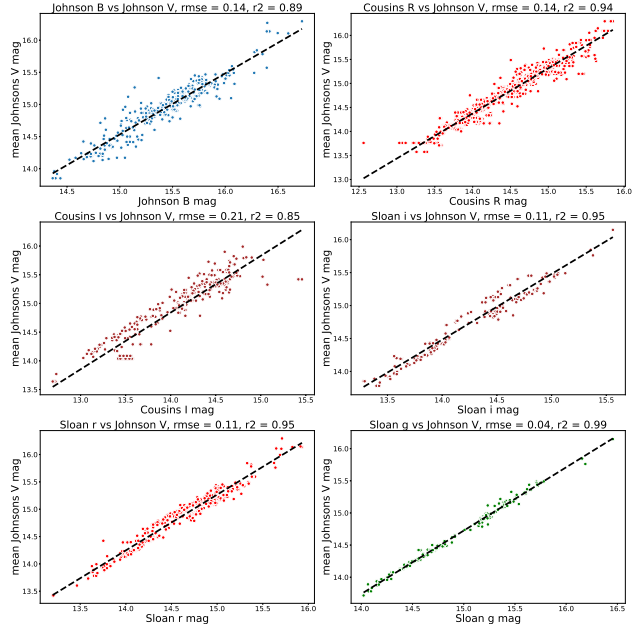


Figure 4: Calibration diagrams of the transition from alternative filters to Johnsons V and corresponding regressions

the optical and radio bands, wavelet analysis based on the Weighted Wavelet Z-Transform (WWZ) was applied, which is proposed by Foster (1996) as a wavelet transformation method for non-uniform time series. The Wavelet Transform allows to localize periods not only in frequency domain, but also in time (in contrast to the spatially/temporally global Fourier analysis). The python library libwwz (ISLA Group, University of Hawaii, 2025), which provides a robust interface for WWZ computation, was used to perform the transformation. In general, this allows to study both stable (constantly present in the signal) and temporary or evolving periods, which is critically important when studying stochastic signals such as radio fluxes or AGN light curves.

As an additional validation metric in the time-frequency analysis, the Lomb–Scargle method was used, which is a classic method for detecting periodic-

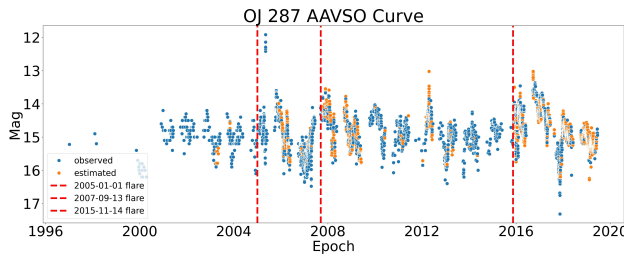


Figure 5: The full light curve, including actual observations in Johnson V (blue), approximate values based on other filters (orange), and dates of flares that fall within the corresponding range of observations (red).

ity in signals in non-uniformly distributed time series. Lomb–Scargle is a generalized Fourier transform based on a weighted harmonic approximation with a correction to the mean value (Lomb, 1976 and Scargle, 1982). In this work, the timeseries.LombScargle implementation (Astropy Collaboration, 2025) of the astropy library (Astropy Collaboration et al., 2022) was used. Cross-correlation is used to find time delays and shifts between flares.

For clustering purposes, the work uses the KMeans model, a machine learning algorithm that allows dividing data into a predetermined number of clusters with minimal internal variation by minimizing a loss function known as inertia, the sum of the distances between points in the data and their centroid (Sculley, 2010). For implementation, an implementation using the scikit-learn (2025) python library (sklearn.cluster.KMeans) is used.

3. Results

The wavelet periodogram of the core radio flux (Fig. 6) shows variability over a wide range of periods. In particular, there is a broad and long-lasting peak near ~ 12 yr, which is consistent with the main orbital period of the binary supermassive black hole according to the model described above. The peak at $\sim 6 - 7$ yr is likely a harmonic of this main period. The $\sim 2 - 3$ yr periods correspond to the intervals between flares, particularly in 2005–2007, and have resumed since ~ 2016 , which is consistent with the temporal localization of the corresponding flares. The shorter periods are likely related to stochastic processes in the jet or accretion disk.

In this paper, we discuss the identification of patterns that could hint at a binary black hole in AGN. Thus, we must continue with the analysis of the optical variability, which was the first to hypothesize a binary black hole in OJ 287.

Fig. 7 shows periodograms obtained using the

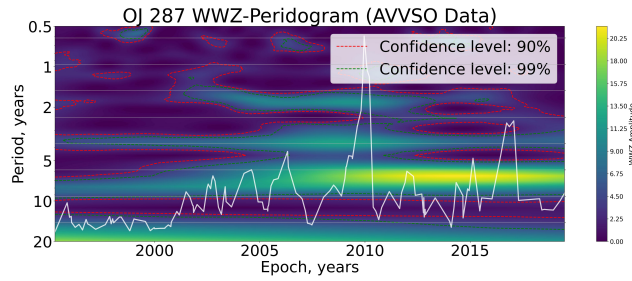


Figure 6: Wavelet periodogram of the radio nucleus OJ 287 with the radio flux curve superimposed (in white).

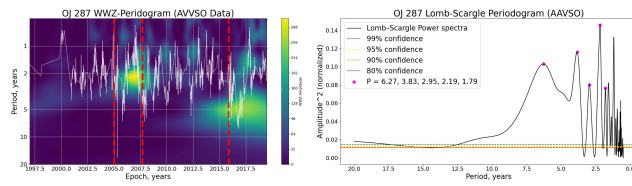


Figure 7: Periodograms: Wavelet with marked flare dates (red lines) — left and Lomb-Scargle with confidence levels (right).

wavelet transform (WWZ) and the Lomb-Scargle method, based on AAVSO optical observations, reduced to a single filter and averaged daily. The detected quasi-periods of variability alone, without additional context, provide limited interpretation. However, in combination with the already known main period (~ 12 yr), which manifests itself in both periodograms as a harmonic with a period of ~ 6 yr, the picture becomes obvious. In particular, it is worth noting the peaks in the wavelet periodogram — bursts with a period of $\sim 2 - 3$ yr, which are well consistent in time between consecutive OJ 287 flares and their dates. All this is also well confirmed by the Lomb-Scargle periodogram.

The light curves corresponding to the flares in the time interval considered in this work are shown in Fig. 8. Fig. 5 shows that the flare of late 2015 is the best described, so we will choose it as the basis for patterning. However, to validate the repeatability of the pattern, we will compare the corresponding light curve with two others using cross-correlation. The result of optimal superposition in this way can be seen in Fig. 9.

Thus (Fig. 9) the pattern of flares is at least approximately repeatable: all the curves considered exhibit a characteristic asymmetric morphology: rapid growth, a secondary (weaker) peak and a long slow decline within approximately the same time scales. This highlights the possibility of finding similar patterns in other binary black hole candidates in AGN, although the final verification of OJ 287-like systems will of course require

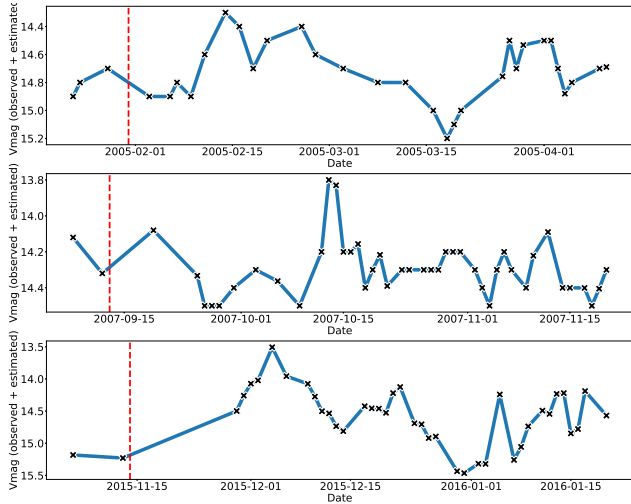


Figure 8: Light curves for the 2005, 2007, and 2015 flares, with daily averages of the data.

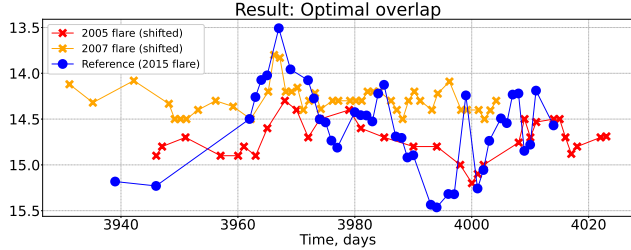


Figure 9: Optimal overlap of the 2015 reference flare (blue) and the 2005 and 2007 flares (red and orange, respectively).

additional statistical tests and simulations.

After the 2007 optical event, a radio-band flare was detected at the end of 2009 (Figs. 1 and 6). As shown in Fig. 10, the range of component position angles becomes markedly chaotic following this flare — exhibiting a significant expansion. This behavior suggests the onset of strong perturbations within the jet, likely triggered by the close passage of the secondary black hole and its gravitational impact on both the jet structure and the accretion disk.

To visualize the evolution of the jet component position angles, we employed a polar diagram (Fig. 11), where the radial coordinate corresponds to the observation index (ordered by date), and the angular coordinate represents the component's position angle. This approach enables tracking the spatiotemporal dynamics of jet morphology. In Fig. 11 (left), the time-angle diagram displays component observations grouped relative to the date of the 2009 radio flare. The same panel (right) also presents automatic clustering in the space $(n, \cos(PA), \sin(PA))$, where

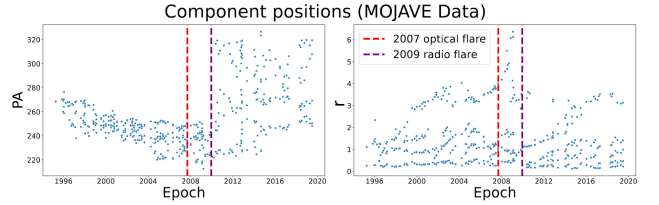


Figure 10: Diagrams of component position angles over time (left) and distances from the nucleus (right) with dates of optical (red) and radio (purple) flares.

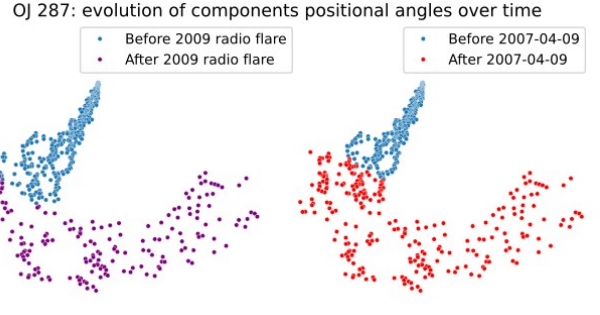


Figure 11: Time-angular visualization of the evolution of position angles of the components of the OJ 287 jet. Left: components grouped by the date of the 2009 radio burst. Right: automatic clustering.

n is the observation index. This clustering reveals the temporal location (distance on the diagram) of jet perturbation — preceding the 2007 flare, which corresponds to the approach of the secondary black hole near the accretion disk. Such a method allows the detection of structural changes in jet morphology without prior assumptions about event timing, and facilitates correlation with optical and radio features.

4. Discussion

We observe the results that we would expect: a clear connection between the temporal dynamics of optical flares, radio emission, and changes in the spatial morphology of the OJ 287 jet. Our analysis is consistent with the key tenets of the double SMBH model in OJ 287. In particular, the detection of a quasi-periodicity of about 12 years in the core radio flux is consistent with the orbital period of the secondary black hole. The peaks at 6–7 years are likely to be harmonics or related to the modulation of the accretion disk, as described in the literature.

A critically important result is the detection of a repeating asymmetric pattern of optical flares. This morphology (rapid rise, secondary peak, slow decline) is not typical of stochastic AGN variability, but is con-

sistent with the mechanism of a secondary black hole collision with an accretion disk (superflares) and subsequent accelerated accretion (tidal-induced outbursts). The repeatability of this pattern makes it a powerful indicator for searching for similar systems.

On the other hand, the analysis of changes in the position angles of the jet components (Fig. 10, 11) demonstrates a clear connection between optical events and spatial perturbations in the jet. The expansion of the range of position angles after the 2007/2009 flares indicates a significant gravitational influence of the secondary BH, which changes the conditions for launching and/or collimation of the jet. The clustering result (Fig. 11), which highlights the moment of perturbation before the 2007 optical flare, is particularly indicative. This indicates that the jet dynamics can respond to the approach of the BH companion to the accretion disk earlier than the impact/flare itself occurs in the optical range.

This time lag between the change in jet morphology, optical flare, and radio burst confirms a complex cascade of physical processes: companion approach/impact, perturbation of the accretion disk and jet; gas perturbed by the impact cools: optical flare occurs (with a delay); accretion onto the main black hole intensifies; jet activation occurs (delayed radio burst).

Limitations: The established correlations are based on a phenomenological analysis of a single object (OJ 287). To verify the reliability of these indicators (asymmetric optical pattern + characteristic change in jet angles), their application to a wider sample of AGN with signs of binarity (e.g. light curves with a periodicity of 1-10 years) is necessary. In addition, for a more accurate modeling of the transition between filters in AAVSO, nonlinear regression models or color indices should be considered.

5. Conclusions

1. Key periods of variability have been confirmed: the WWZ and Lomb–Scargle methods have detected quasi-periods of about 12 years in the radio fluxes and optical light curve of OJ 287 and its harmonics, which is consistent with the orbital period of the secondary BH.

2. A repeating pattern of optical flares is shown: light curves corresponding to periods of activity exhibit a clear asymmetric morphology (rapid rise, secondary peak, slow decline). This pattern is a characteristic manifestation of a BH companion collision with an accretion disk.

3. The relationship between optical and radio flares and jet morphology is shown: the period of optical and radio flares correlates with the appearance of significant, chaotic perturbations in the OJ 287 jet, which manifest themselves in the expansion of the range of

position angles of bright components.

4. A criterion for identifying candidates has been formulated: the presence of periodicity in optics and radio with corresponding periods, characteristic asymmetric flashes in optics, a change in the orientation of components, and corresponding radio flares.

Acknowledgements. We acknowledge with thanks the variable star observations from the AAVSO International Database contributed by observers worldwide and used in this research. This research has made use of data from the MOJAVE database that is maintained by the MOJAVE team [Lister et al. 2018]. This research has made use of the VizieR catalogue access tool, CDS, Strasbourg, France (DOI: 10.26093/cds/vizier). The original description of the VizieR service was published in 2000, A&AS 143, 23.

References

Alachkar A., Ellis J., Fairbairn M.: 2023, *Phys. Rev. D*, **107**, 103033.

American Association of Variable Star Observers (AAVSO): 2025, <https://www.aavso.org/>

Astropy Collaboration: 2025, <https://docs.astropy.org/en/stable/api/astropy.timeseries.LombScargle.html>

Astropy Collaboration, Price-Whelan A.M., Lim P.L. et al.: 2022, *Astrophys. J.*, **935**, 167.

Dey L., Gopakumar A., Valtonen M. et al.: 2019, *Universe*, **5**, 108.

Foster G.: 1996, *Astron. J.*, **112**, 1709.

ISLA Group, University of Hawaii: 2025, <https://github.com/ISLA-UH/libwwz>

Komossa S., Grupe D., Parker M.L. et al.: 2021, *Mon. Not. R. Astron. Soc.*, **504**, 5575–5587.

Laine S., Dey L., Valtonen M. et al.: 2020, *Astrophys. J. Lett.*, **894**, L1.

Lehto H.J., Valtonen M.J.: 1996, *Astrophys. J.*, **460**, 207.

Lister M.L., Aller M.F., Aller H.D. et al.: 2018, *Astrophys. J. Suppl. Ser.*, **234**, 12.

Lister M.L., Homan D.C., Hovatta T. et al.: 2019, *Astrophys. J.*, **874**, 43.

Lister M.L., Homan D.C., Kellermann K.I. et al.: 2021, *Astrophys. J.*, **923**, 30.

Lomb N.R.: 1976, *Astrophys. Space Sci.*, **39**, 447–462.

Marscher A.P.: 2009, <https://arxiv.org/abs/0909.2576>

MOJAVE Team: 2025, <https://www.cv.nrao.edu/MOJAVE/allsources.html>

NASA/IPAC Extragalactic Database: 2008, <http://ned.ipac.caltech.edu/cgi-bin/objsearch?objname=OJ+287>

Ochsenbein F.: 1996, <https://vizier.cds.unistra.fr>

Scargle J.D.: 1982, *Astrophys. J.*, **263**, 835.

Scikit-learn developers: 2025, <https://scikit-learn.org/stable/modules/generated/sklearn.cluster.KMeans.html>

Sculley D.: 2010, *Proc. 19th Int. Conf. World Wide Web*, 1177–1178.

Sillanpaa A., Haarala S., Valtonen M.J. et al.: 1988, *Astrophys. J.*, **325**, 628.

Sillanpaa A., Takalo L.O., Pursimo T. et al.: 1996, *Astron. Astrophys.*, **315**, L13–L16.

Sundelius B., Wahde M., Lehto H.J. et al.: 1997, *Astrophys. J.*, **484**, 180–185.

Valtonen M.J., Lehto H.J.: 1997, *Astrophys. J.*, **481**, L5–L7.

Valtonen M.J., Lehto H.J., Sillanpaa A. et al.: 2006, *Astrophys. J.*, **646**, 36–48.

Valtonen M.J., Mikkola S., Merritt D. et al.: 2010, *Astrophys. J.*, **709**, 725–732.

Valtonen M.J., Nilsson K., Villforth C. et al.: 2009, *Astrophys. J.*, **698**, 781–785.

Valtonen M.J., Zola S., Ciprini S. et al.: 2016, *Astrophys. J. Lett.*, **819**, L37.

Zabora D., Ryabov M., Sukharev A. et al.: 2022, *Astron. Astrophys. Trans.*, **33**, 89–100.

Zabora D., Ryabov M., Sukharev A. et al.: 2023, *Odessa Astron. Publ.*, **36**, 154–160.

Zabora D., Ryabov M., Sukharev A.: 2025, *Astron. Astrophys. Trans.*, **34**, 343–362.